Cyclic Fatigue Model

Ibsen, Lars Bo

Publication date:
1999

Document Version
Publisher's PDF, also known as Version of record

AAU Geotechnical Engineering Papers ISSN 1398-6465 R 9916

Cyclic Fatigue Model

L.B. Ibsen

1999 Soil Mechanics Paper No 34

GEOTECHNICAL ENGINEERING GROUP
AALBORG UNIVERSITY DENMARK

Ibsen, L.B. (1999). Cyclic Fatigue Model.

AAU Geotechnical Engineering Papers, ISSN 1398-6465 R9916.

Soil Mechanics Paper No 34

The paper has been published in

The **A**AU **G**eotechnical **E**ngineering **P**apers - AGEP - are issued for early dissemination and book keeping of research results from the Geotechnical Engineering Group at Aalborg University (Department of Civil Engineering). Moreover, the papers accommodate proliferation and documentation of field and laboratory test series not directly suited for publication in journals or proceedings.

The papers are numbered ISSN 1398-6465 R<two digit year code><two digit consecutive number>. For internal purposes the papers are, further, submitted with coloured covers in the following series:

Series	Colour
Laboratory testing papers	sand
Field testing papers	grey
Manuals & guides	red
Soil Mechanics papers	blue
Foundation Engineering papers	green
Engineering Geology papers	yellow
Environmental Engineering papers	brown

In general the AGEP papers are submitted to journals, conferences or scientific meetings and hence, whenever possible, reference should be given to the final publication (journal, proceeding etc.) and not to the AGEPpaper.

Cyclic Fatigue Model

Lars Bo Ibsen

Soil Mechanics Laboratory, Aalborg University, Denmark

1 Introduction

The cyclic fatigue model described in this paper has been developed in the light of the "Cyclic fatigue theory for sand" as described in /Ibsen, L.B., 1993/. The model determines the stress development during cyclic loading. Compared to other cyclic models, which normally describe development of stress/strain using *Stress Ratio* defined as

$$\eta = \frac{q'}{p'} \tag{1}$$

see for instance /Hydro, M. et al. 1991/, this model describes the stress/strain development in a normalized stress space defined by the *Mobilization Index*, see section 1.1. Applying the mobilization index causes the stress state to be normalized regarding the strength of the soil and the model is independent of the stress level and the strength of the sand, contrary to models where Stress Ratio is applied. The model in /Jacobsen, M. and Ibsen, L.B. 1991/ can be regarded as a first order theory describing the stress/strain development applying the theory of elasticity. The model, described in this paper, has been further developed in order to be able to model the stress developments moving towards failure. Thus, the non-linearities have been introduced in the model.

1.1 Mobilization index

The test results are transformed from the stress space, defined by p', q', to the normalized stress space by introducing the *Mobilization index M*

$$M = \frac{q'}{|q'_f(p')|} \quad ; \quad -0.69 < M < 1 \tag{2}$$

where q' and q'_f are determined at the same mean stress p', see Figure 1. When the stress state moves towards failure in triaxial tension, line failure will develop even in tests with equal height and diameter of the specimen. Since the failure condition in tension hereby is "unknown", it has been decided to normalize the entire stress space by the failure condition

in compression. This causes Cyclic Liquefaction to occur for $M = 1$ and Necking to occur for $M = -0.69$.

In /Ibsen, L.B., 1993/ it has been shown that the position of the drained anisotropic stress state (p'_s, q'_s) – compared to the stable cyclic line – governs the stress development in cyclic tests. The stable cyclic line, SCL, is characterized by a constant value M_s in the normalized stress space, see Figure 1. The drained anisotropic stress state - just before cyclic loading - is defined by the *Start Mobilization Index* M°_m as

$$M^\circ_m = \frac{q'_s}{q'_f(p'_s)} \tag{3}$$

In the normalized stress space, the stress development during the cyclic loading is characterized by the development of the mobilization index as a function of the number of cycles. Figure 1b shows that the stress development can be described by the development of the *Maximum Mobilization Index* M_{max} and the *Mean Mobilization Index* M_m as a function of the number of cyclic loadings. M_{max} is determined as the maximum value of the mobilization index of each individual cycle while M_m is determined as

$$M_m = \frac{q'_m}{q'_f(p'_m)} \tag{4}$$

The suffix m indicates mean valve of the cycle.

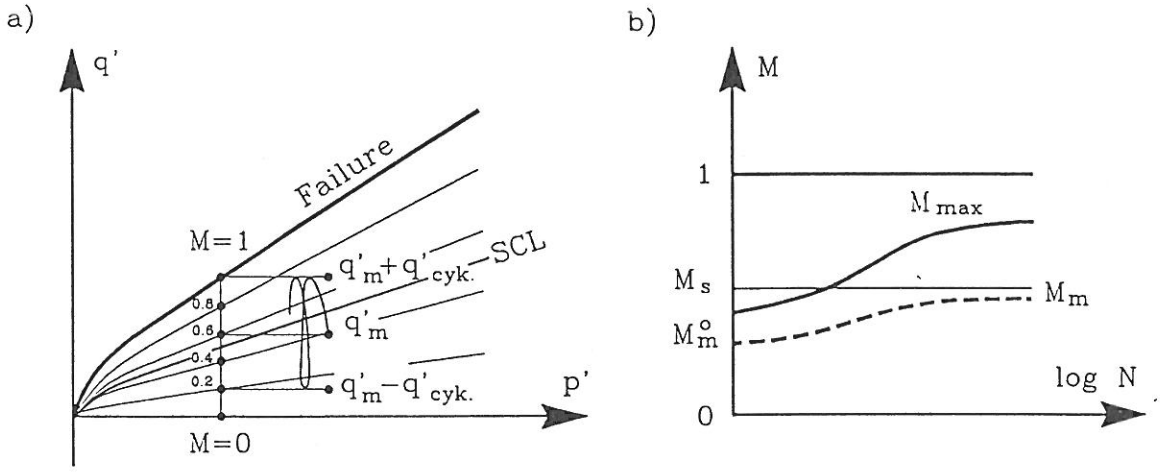

Figure 1. Transformation of the test results from the stress space p', q' to the normalized stress space M. a) Normalization of q'. b) The normalized stress space M.

Since the entire stress space is normalized by the failure condition in compression, $M(+q'(p'))$ $= |M(-q'(p'))|$. This causes the mobilization index to be developed symmetrically around M_m for cycles where $q'_{min} < 0$. It would not be the case if the tensile stresses were normalized by the failure condition in tension. This symmetry is a great advantage for the numerical modelling. During dimensioning the only interesting part is to be able to describe the development of stress until failure, i.e. in cyclic triaxial tests when Butterflies start to develop.

if the minimum stress level q'_{min} exceeds the characteristic line in extension CL^- after a number of cycles, see Figure 2. The pore pressure generation δu will go from $\delta u > 0$ to $\delta u < 0$ twice during each cycle and the equilibrium of the stable state cannot be created. After the minimum stress level q'_{min} has exceeded the characteristic line in extension CL^-, the drained failure envelope will be reached during the subsequent cycle. Cyclic Liquefaction as defined by Casagrande (1971) will be observed if the maximum stress level q'_{max} reaches the drained failure envelope in compression during the subsequent cycle. Necking, which is a similar phenomenon to Cyclic Liquefaction and defined by Casagrande (1971), will be observed if q'_{min} reaches the drained failure envelope in extension. Thus, the characteristic line in extension CL^- can be defined as a failure indicator. The failure indicator is introduced in the model as the fatigue boundary, which means that the cyclic failure condition will develop if

$$M_{min} \leq M_{cl-} \tag{5}$$

M_{min} is the smallest value of the mobilization index of the individual cycle. M_{cl-} is the failure indicator, which for $q'_{min} < 0$ in Figure 2, can be determined as

$$M_{cl-} = \frac{q'_{min}}{q'_f(p'_{cl-})} \tag{6}$$

where

$$p'_{cl-} = \frac{q'_{min}}{tan\varphi_{cl-}} \tag{7}$$

For Lund Sand No 0, see /Ibsen, L.B., 1993/, $tan\varphi_{cl-}$ is determined as

$$tan\varphi_{cl-} = -0.846 \tag{8}$$

According to /Ibsen, L.B., 1993/ the friction capacity in compression is determined under homogeneous conditions. Since the friction capacity in tension was observed to be identical with the condition in compression, it is postulated that

- If $M_{min} > M_{cl-}$, homogeneous conditions will prevail in the test for $q'_{min} < 0$.

Applying M_{cl-} as failure indicator, the stress/strain development until failure is observed to be determined from homogeneous conditions in the sand. However, it is of no interest modelling the stress/strain development after failure has developed in the soil. Thus, M_{max} in the model is assessed as

$$M_{max} = 1 \quad \text{for} \quad M_{min} \leq M_{cl-}$$

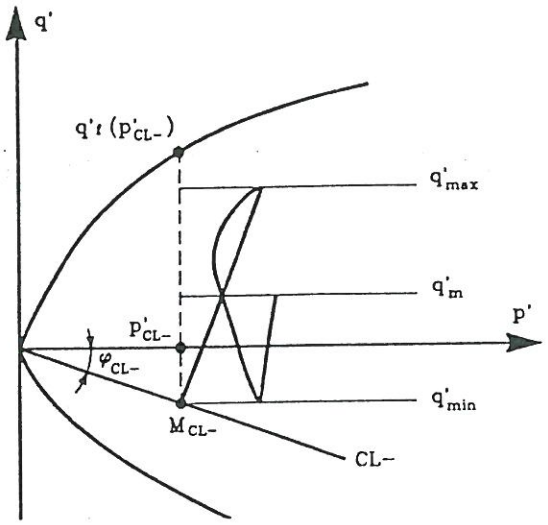

Figure 2. Determination of M_{cl-}.

Subsequently the cyclic fatigue theory can be formulated.

- If $M_m^\circ < M_s$ and $M_{max} < 1$, the phenomenon Mobilization will develop, see Figure 3a.
- If $M_{min} < M_{cl}$ during the pore pressure buildup, cyclic failure will occur. In Figure 3b M_{max} takes the value 1 and failure occurs as Cyclic Liquefaction.
- If $M_m^\circ > M_s$ negative pore pressure will be generated and Stabilization will develop, see Figure 3c.

If M_m during the initial cycle goes from being larger than M_s to being smaller than M_s, Instant Stabilization will develop. In the model Instant Stabilization is treated as Mobilization since M_m° is defined from the value of p'_m, q'_m in the initial cycle.

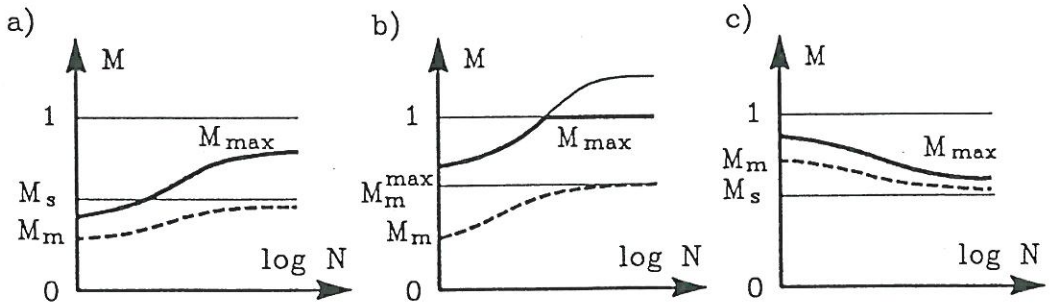

Figure 3. The development of the mobilization index by the phenomena a) Mobilization, b) Cyclic Liquefaction, c) Stabilization. The tests have been described by the development of the maximum mobilization degree M_{max} and the mean mobilization degree M_m.

Applying the mobility index instead of the stress ratio in the cyclic fatigue model has the following advantages:

- The mobilization index makes it possible to compare tests performed with different densities and different types of sand, since q' is normalized with respect to the strength of the soil.
- The mobilization index may be used whether the limitation of the stress space is described as a pure friction material, a Coulomb material, or a curved failure envelope is applied.
- The mobilization index can be applied in a mathematical formulation which describes the hysterese behaviour of the material even at large strains and in complicated stress variations, see Figure 4.

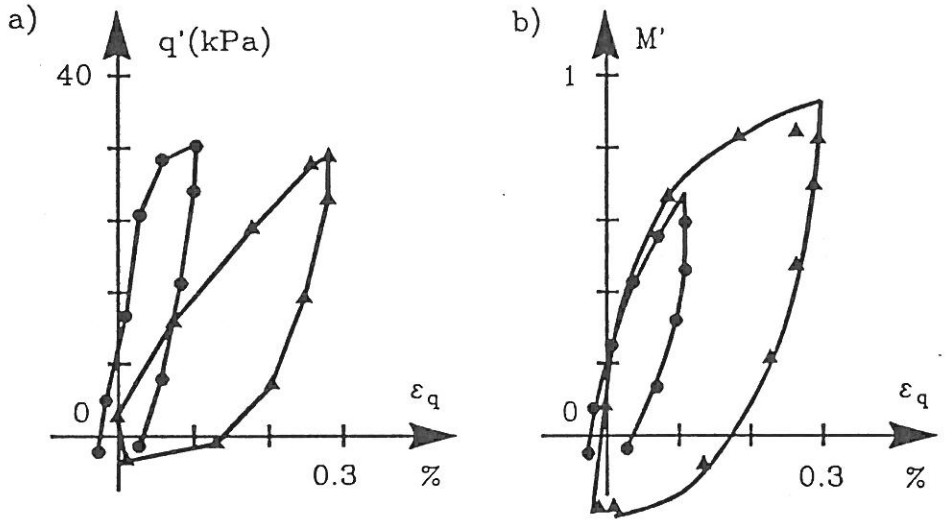

Figure 4. Normalizing the stress space using the mobilization index, the hysteresis behaviour can be modelled, even with complicated stress- and strain variations.

Modelling the development of M_m, M_{min} and M_{max} as functions of the number of cyclic loadings, the stress development can be described in the cyclic test.

1.2 Description of M_m

The development of the mean mobilization index M_m as function of the number of cyclic loadings can be described in a simple way as

$$M_m = M_m^\circ + (M_m^\infty - M_m^\circ)\, f(N) \tag{9}$$

M_m^∞ is the mobilization index which M_m moves towards for $N \to \infty$. In agreement with the fatigue theory, M_m^∞ assesses the value of M_s or M_m^{max}. Figure 3 shows that Mobilization

and Stabilization move towards the stable cyclic line M_s while M_m moves towards M_m^{max} in Cyclic Liquefaction corresponding to the fact that the compression part of the cycle follows the failure envelope, see Figure 5. In (9) $f(N)$ governs the curvature and the speed in which $M_m \rightarrow M_m^{\infty}$. $f(N)$ must comply with the following boundary conditions

$$f(N) = 0 \qquad \text{for} \qquad N = 0$$

$$f(N) \rightarrow 1 \qquad \text{for} \qquad N \rightarrow \infty$$

A function which complies with these condition is

$$f(N) = \left(\frac{N}{N + N_0}\right)^{\ell} \tag{10}$$

In order to apply this equation system in (9) and (10) it is necessary to be able to determine the constants M_m^{∞}, N_0 and ℓ from the initial conditions of the cyclic loadings, i.e. the drained, anisotropic stress state (p'_s, q'_m), just before cyclic loading and the cyclic amplitude q'_{cyk}.

Determination of M_m^{∞}

p', q' plottings in Figure 9 /Ibsen, L.B., 1993/ show that the inclination of the cycle changes throughout the test. The inclination of the cycles varies from $\alpha = 0$ to $\alpha = \varphi_s$, see Figure 5. If α takes the value 0 the material can be considered to be elastic, which is only the case when $M_{max}/M_m \approx 1$. Figure 5 shows that $\alpha \rightarrow \varphi_s$ for $M_{max} \rightarrow 1$, which means that the material can be considered to be plastic, since the compression part of the cycle follows the drained failure condition. It is also observed that $M_m \rightarrow M_m^{max}$ for $M_{max} \rightarrow 1$. M_m^{max} can be determined as

$$M_m^{max} = \frac{q'_m}{q'_f(p'^{min}_m)} \tag{11}$$

p'^{min}_m is a function of q'_{max} given by

$$p'^{min}_m = \frac{q'_m}{tan\varphi_s} \tag{12}$$

since

$$tan\varphi_s = \frac{q'_{\varphi_s}}{p'_{\varphi_s}} = \frac{q'_{max}}{p'_{\varphi_s}} \tag{13}$$

and

$$p'^{min}_m = \frac{p'_{\varphi_s}}{2} \tag{14}$$

From equation (15) and (13) $tan\varphi_s$ can be found

$$q'_f = \frac{6\ sin\varphi_a}{3 - sin\varphi_a}\left(1 + \frac{c_a \cdot cot\varphi_a}{m \cdot p'}\right)^m \tag{15}$$

$$tan\varphi_s = \left(\frac{q'_{max}}{(\frac{6sin\varphi_a}{3-sin\varphi_a})^{\frac{1}{m}} \cdot \frac{c_a cot\varphi_a}{m}} \right)^{\frac{m}{m-1}} \tag{16}$$

since the right order term

$$\frac{1}{(tan\varphi_s)^{\frac{1}{m}}} \approx 0 \tag{17}$$

has been omitted. Equation (15) describes the curved failure lines. The suffix a indicates asymptotic parameters. m describes the curvature of the failure lines.

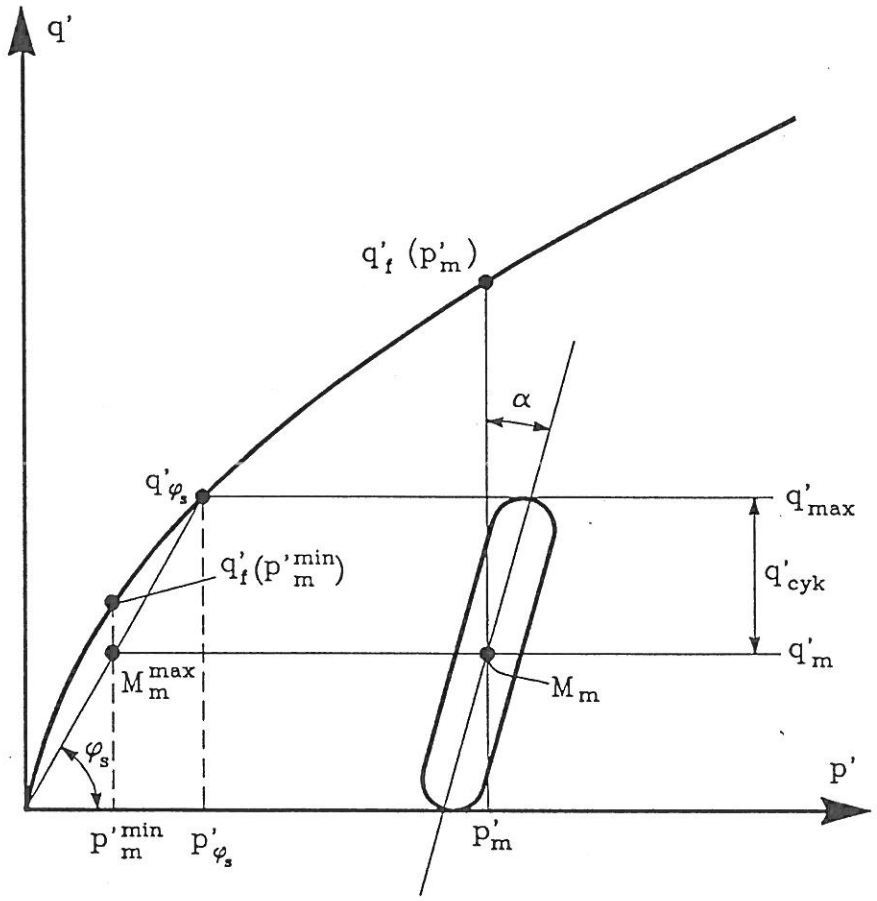

Figure 5. Determination of M_m^{max}.

It is postulated that a yield indicator M_y exists which is defined

$$M_y = k_q M_s \tag{18}$$

$$k_q = \frac{q'_m + q'_{cyk}}{q'_m} \tag{19}$$

k_q is the amplitude ratio defined from the deviator stresses q'_m and q'_{cyk}. The amplitude ratio is determined from the initial parameters of the cyclic loading and remains constant

throughout the entire test, even though $\alpha \rightarrow \varphi_s$, see Figure 5. For elastic material, i.e. $\alpha = 0$, M_y will be equal to M_{max} and k_q can be found

$$M_{max} = \frac{q'_{max}}{q_f} = \frac{q'_m + q'_{cyk}}{q'_f} \tag{20}$$

from (4) it is observed that

$$q'_f = \frac{q'_m}{M_m} \tag{21}$$

$$M_{max} = \frac{q'_m + q'_{cyk}}{q'_m} M_m = k_q M_m \tag{22}$$

According to the failure hypothesis in /Ibsen, L.B., 1993/ it is possible to determine that

$M_y > 1 \Rightarrow$ develops failure

$M_y \leq 1 \Rightarrow$ develops a stable cyclic state

The value of M_m^∞, which is applied in the simulation, can now be determined from the initial parameters of the cyclic loading as

- $M_y > 1$ is $M_m^\infty = M_m^{max}$
- $M_y \leq 1$ is $M_m^\infty = M_s$

M_m^{max} is determined from (11) and M_s is determined in the following parameter determination.

Parameter determination

In cyclic triaxial tests M_m^0, M_m^{max} are normally known whereas M_s, N_0 and ℓ are variables. However, the main part of the 87xx tests are performed by applying q'_{cyk} increasingly, so that the chosen value is reached around cycle 2 - 3. This test procedure was applied at a time when the mechanisms governing the development of pore pressure had not yet been clarified. The test procedure was introduced in order to avoid the phenomenon Instant Stabilization, which at the time was interpreted as being a result of applying q'_{cyk} too momentarily, since Δu in some cases was observed to be negative and not positive as expected during the initial cycle. The effect of the initial 2 - 3 cycles has been determined from the curvature of the remaining cycles, i.e. M_m^0 is determined by curve fitting. In the curve fitting procedure 4 unknown quantities per test must be determined. The 4 parameters converge with very different speed, which makes parameter fitting virtually impossible in one procedure. The fast converging parameters will dominate the effect of the slow converging parameters. The domineering parameters are found by the difference $(M_m^\infty - M_m^0)$ determining the stress development, see Figure 6. During the curve fitting of Mobilization-, Stabilization- and Instant Stabilization tests it is evident that M_s converges fastest, since at least 200 cycles assume this value. M_m^0 determines the slow part of the curvature and converges reasonably.

N_0 is the "speeder" with which the velocity of the stress development can be adjusted, see Figure 7, and ℓ, which determines the shape of the curve, see Figure 8. These parameters are difficult to determine since they are mutually dependent according to (10). The 4 unknown parameters are determined by the method of least squares, applying the following step by step procedure in each test:

1. M_s is fitted. $\ell = 1$ and M_m^0, M_s and N_0 is varied.
2. ℓ is fitted, applying M_m^0 and M_s as determined according to 1. ℓ and N_0 are varied.
3. M_m^0 is fitted, applying M_s according to 1 and ℓ according to 2. M_m^0 and N_0 are varied.
4. N_0 is fitted, applying M_s, ℓ and M_m^0 determined in 1 - 3. N_0 is varied.

In the following section the result of this step by step fitting will be commented on. The results are shown in Tables 1 and 2.

Test	e_o	k_q	M_m°	M_s	N_o	$M_s - M_m^\circ$	$\frac{\text{Error}^2}{\text{No.of cyc.}}$	Classification
8713**)	0.623	2.15	0.225	0.435	23	0.21	1.6E-05	Mobilization
8714**)	0.619	2	0.26	0.5	24	0.24	1.7E-05	Mobilization
8719**)	0.617	1.65	0.48	0.54	12	0.06	8E-06	Mobilization
8720**)	0.618	1.78	0.42	0.525	15	0.105	7E-06	Mobilization
8726**)	0.62	1.9	0.395	0.475	12	0.08	1E-05	Mobilization
8728**)	0.61	2	0.305	0.445	18	0.14	3.3E-05	Mobilization
8729**)	0.614	2.25	0.275	0.475	19	0.2	5E-06	Mobilization
8730**)	0.606	1.52	0.485	0.505	8	0.02	1.1E-05	Mobilization
8732**)	0.625	2.22	0.26	0.445	17	0.185	2.1E-05	Mobilization
8740	0.605	1.82	0.33	0.51	20	0.18	5.2E-05	Mobilization
8800	0.625	1.33	0.34	0.4	13	0.06	1E-05	Mobilization
8802	0.626	1.22	0.485	0.5	11	0.015	2E-06	Mobilization
8807**)	0.608	1.62	0.42	0.475	12	0.055	1.4E -04	Mobilization
8811**)	0.606	2.23	0.33	0.445	14	0.115	2.3E-05	Mobilization
8815**)	0.607	1.83	0.37	0.465	17	0.095	5.8E-05	Mobilization
8709	0.611	1.62	0.535	0.51	10	−0.025	1.2E-05	Stabilization
8809**)	0.611	1.62	0.57	0.51	8	−0.06	5.7E-05	Stabilization
8731*)	0.62	1.43	0.675	0.605	5	−0.07	5E-05	Stabilization
8806*)	0.599	1.29	0.775	0.72	3	−0.055	5E-06	Stabilization
8816*)**)	0.61	1.81	0.56	0.455	5	−0.105	1.6E-05	Stabilization
8810	0.602	1.42	0.515	0.53	8	0.015	1E-05	Instant Stabilization
8812	0.61	2.19	0.505	0.4	0	−0.105	1.5E-05	Instant Stabilization
8813	0.603	1.68	0.66	0.6	3	−0.06	1.2E-05	Instant Stabilization
8814	0.611	1.87	0.335	0.375	11	0.04	9E-06	Instant Stabilization
8818**)	0.6	1.88	0.45	0.495	11	0.045	1.3E-05	Instant Stabilization

Table 1. Results of parameter fittings in tests where $M_Y < 1$.
The tests have been fitted with $\ell = 1.25$.

*) Tests where $\ell = 0, 1$. The main part of M_m's change occurs during the initial cycle.

**) Tests applied for determination of k_m.

Test	e_o	k_q	M_m°	M_m^{max}	N_o	$M_s - M_m^\circ$	$\frac{\text{Error}^2}{\text{No.of cyc.}}$	Classification
8727**)	0.616	2.25	0.335	0.655	27	0.32	5.3E-05	Cyclic Liquefaction
8733	0.639	2.25	0.23	0.82	17	0.59	7.1E-05	Cyclic Liquefaction
9280**)	0.611	2.39	0.322	0.525	15	0.203	7E-06	Cyclic Liquefaction

Table 2. Results of parameter fittings in tests where Cyclic Liquefaction occurs.

**) Tests applied for determination of k_m.

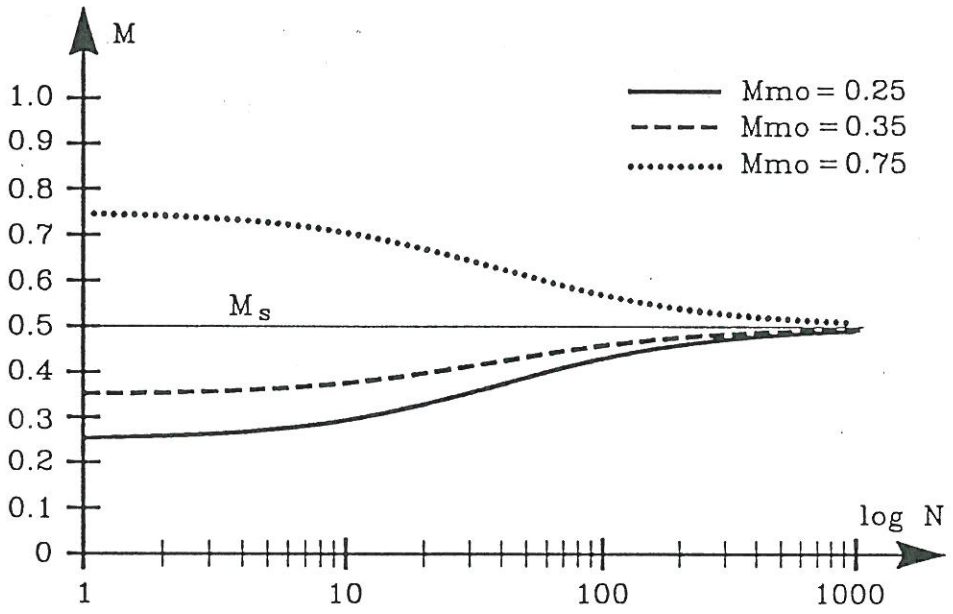

Figure 6. M_m° *determines the stress development from the cyclic strain while the difference* $(M_m^{\max} - M_m^\circ)$ *describes the maximum fatigue which can be developed. The curves in the figure have been determined by (9) and (10), where* $M_s = 0.5$, $N_o = 30$, $\ell = 1.25$.

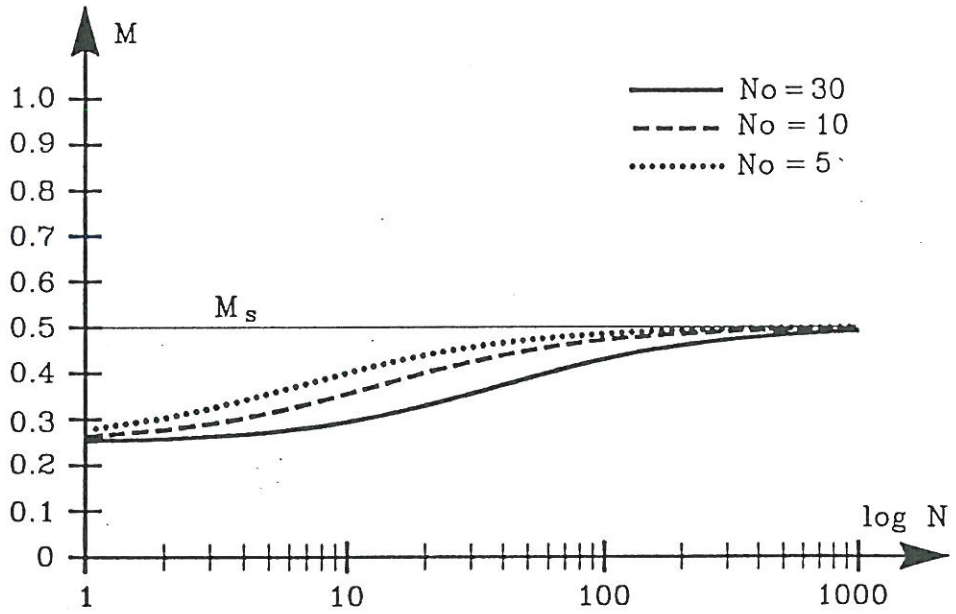

Figure 7. N_o *is the "speeder" controlling the speed with which the stress development takes place. The curves in the figure have been determined by (9) and (10), where* $M_s = 0.5$, $M_m^\circ = 0.25$, $\ell = 1.25$.

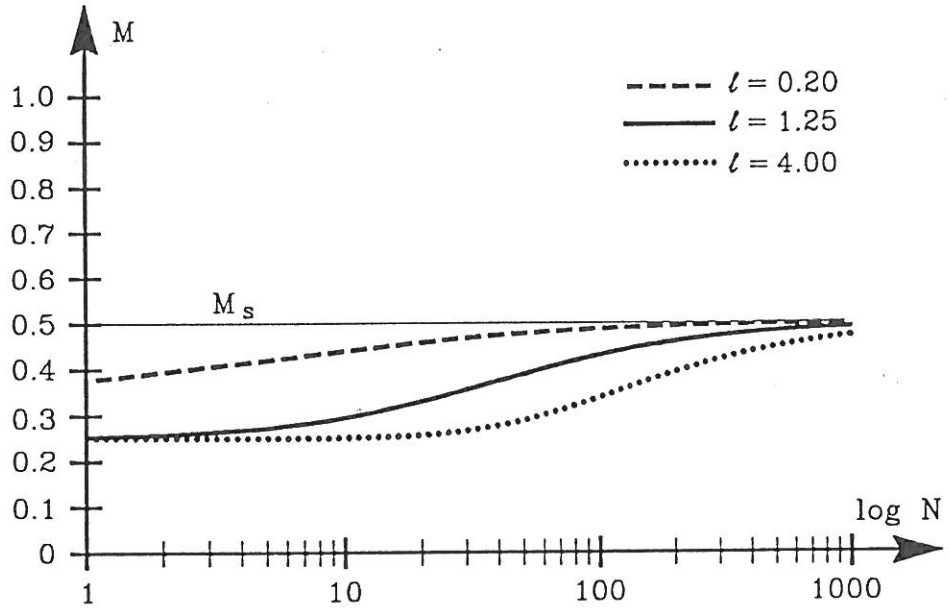

Figure 8. ℓ describes the curvature. The curves in the figure have been determined by (9) and (10), where $M_s = 0.5$, $M_m^\circ = 0.25$, $N_o = 30$.

Determination of M_s

In Figure 9 the distribution of the values for M_s from Table 1 are plotted. Assuming the distribution to be normal it can be determined that

- The mean value of the M_s sample: 0.494.
- Standard deviation of the M_s sample: 0.072.

The hypothesis that M_s is a normal distribution has been tested in a χ^2 test. The hypothesis cannot be rejected on a 21% significant level.

Even though M_s has been fitted in tests where the stable cyclic state has not been fully developed, the mean value of M_s is identical with the SCL line determined in /Ibsen, L.B., 1993/. Consequently, it is concluded that

- $M_s = 0.5$.

On the basis of the available statistical material it cannot be rejected that the mean value of $M_s = 0.5$. Repetition of 25 tests showed the mean value to be placed in the confidence interval $0.46 < M_s < 0.52$ in 95% of the samples.

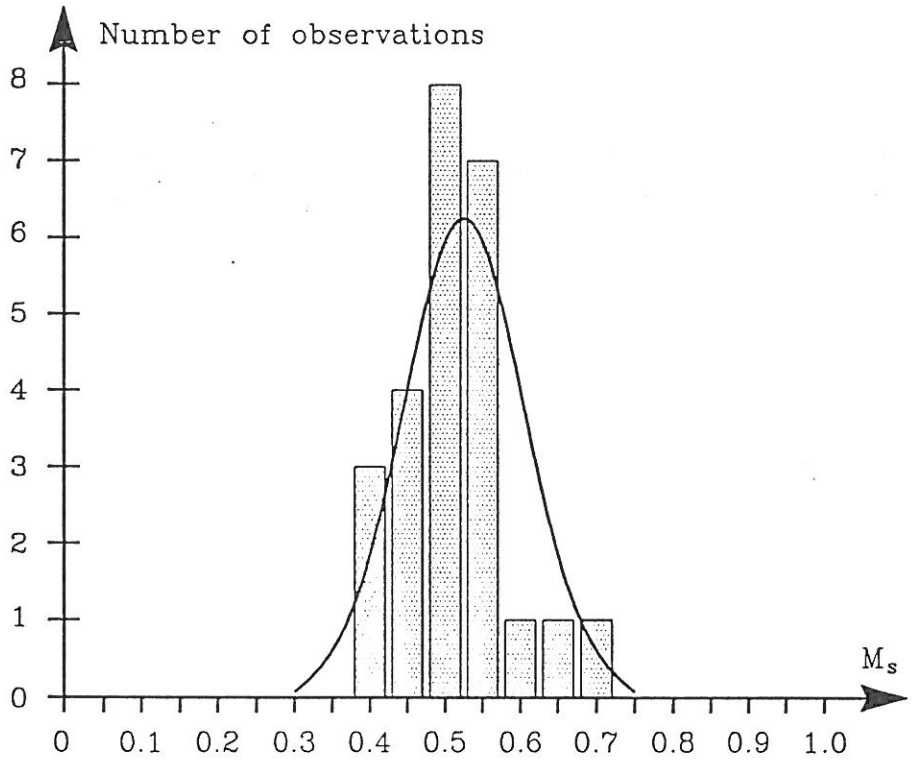

Figure 9. The distribution of the fitted M_s-values.

Determination of ℓ

As shown in Figure 8 ℓ determines the curvature of the stress development. If ℓ assumes a low value, for instance 0.2, a cause is described where the change of M_m takes place during the initial cycles, see Figure 8. If ℓ assumes a higher value, for instance 4, the change of M_m takes place with a constant increase which is distributed evenly on all the cycles. A mutual linkage exists between N_0 and ℓ, see equation (10). A parameter study has shown that ℓ is the least likely of the 4 parameters to contribute to the collected rms. error. In several of the tests the rms. error is constant for $0.5 < \ell < 2$. Thus, it has been decided to let ℓ assume a constant value and adjust the curvature applying N_0. Figure 10 shows the fitting of ℓ. The fitting, which has been carried out with steps of 0.05, has resulted in 294 results corresponding to an average of 10 results per test with the identical rms. error. If the samples are considered to be distributed normally, the result of the fitting can be characterized as follows:

- The mean value of the ℓ sample: 1.24.
- Standard deviation of the ℓ sample: 0.576.

In a χ^2 test, on 66% significant level, it cannot be rejected that ℓ is distributed normally. In /Jacobsen, M. and Ibsen, L.B./ ℓ was determined at 1.25. When repeating – in 95% of the cases – the samples of the mean value for ℓ will be placed in the confidence interval $1.17 < \ell < 1.31$. Consequently, it is assumed that

- $\ell = 1.25$.

The curvature, appearing with $\ell = 1.25$, is in accordance with the stress progress developed in the tests which are described as Cyclic Liquefaction, Mobilization and Instant Stabilization. In 3 out of 8 tests concerning Stabilization it has been observed that the main part of M_m's change takes place during the initial cycle corresponding to the process described with $\ell = 0.2$ in Figure 8. The curvature with $\ell = 1.25$ is not able to describe the stress process in these tests, see Figure 14b. ℓ has been determined to be 0.1 in the fitting of the tests marked with *) in Table 1. It has not been possible to conclude if Stabilization ought to be described with a different curvature that the rest of the phenomena or if the problems observed are of a technical nature when testing. However, it is most likely a transitory phenomenon between pure Stabilization and Instant Stabilization.

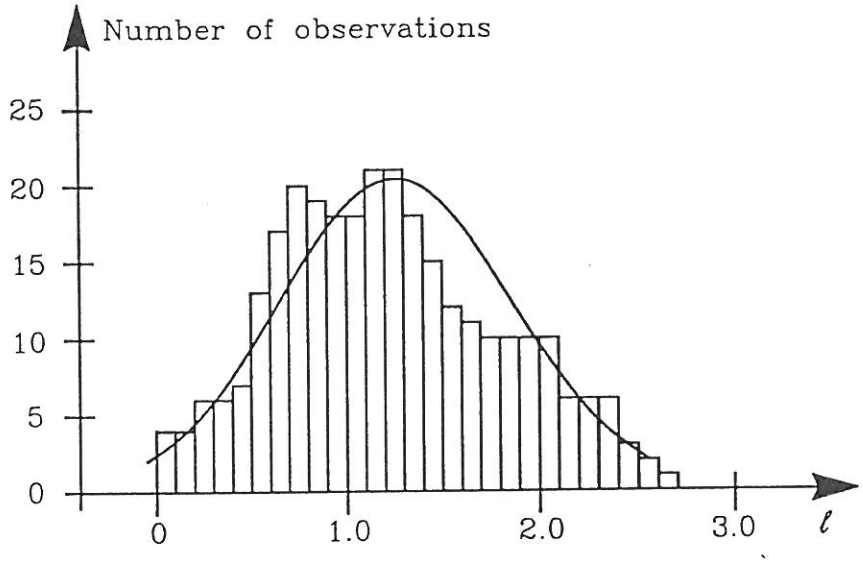

Figure 10. The distribution of the fitting of ℓ

Determination of N_0

As described in Figure 7 N_0 is the "speeder" governing the speed with which $M_m \rightarrow M_m^{\infty}$. The choice $\ell = 1.25$ means that the curvature is locked and adjustment of the curvature can only be made with N_0. Looking at equations (9) and (10) N_0 is expected to be a function of the maximum fatigue $M_m^{\infty} - M_m^{\circ}$, which the cyclicstress variation is able to generate. Since M_m^{∞} is dependent on M_y it has been chosen to describe N_0 as a function of M_m°, see Figure 11. Thus, the function $N_0(M_m^{\circ})$ can be applied to $M_m^{\infty} = M_s$ as well as to $M_m^{\infty} = M_m^{max}$.

The sample of the N_0 fitting is observed to represent an ascending curvature with very little scattering. The tests, which develop Cyclic Liquefaction, Mobilization, Stabilization and Instant Stabilization, can be described by one curve. The function describing the curvature is

$$N_0(M_m^{\circ}) = 8\frac{(1 - M_m^{\circ})}{M_m^{\circ}} \tag{23}$$

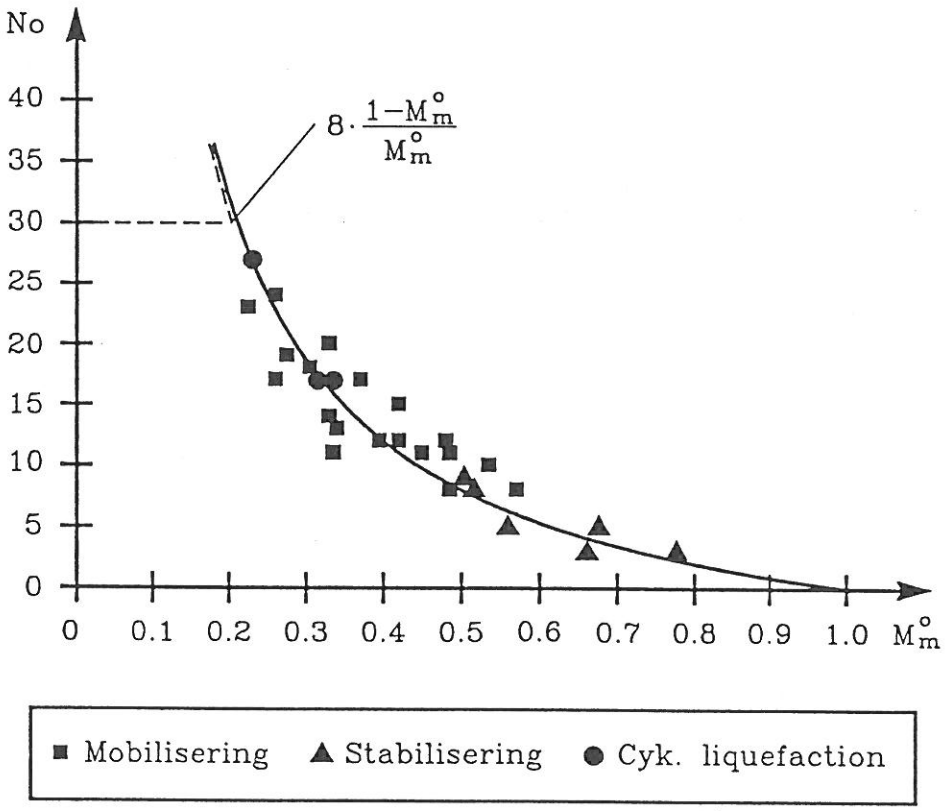

Figure 11. Estimation of N_o as a function of M_m°.

The development of N_0 has not been studied in the tests for $M_m^\circ < 0.2$. Consequently, it cannot be determined if N_0 is to be described by equation (23) in this interval or an upper value for N_0 exists as shown in the figure.

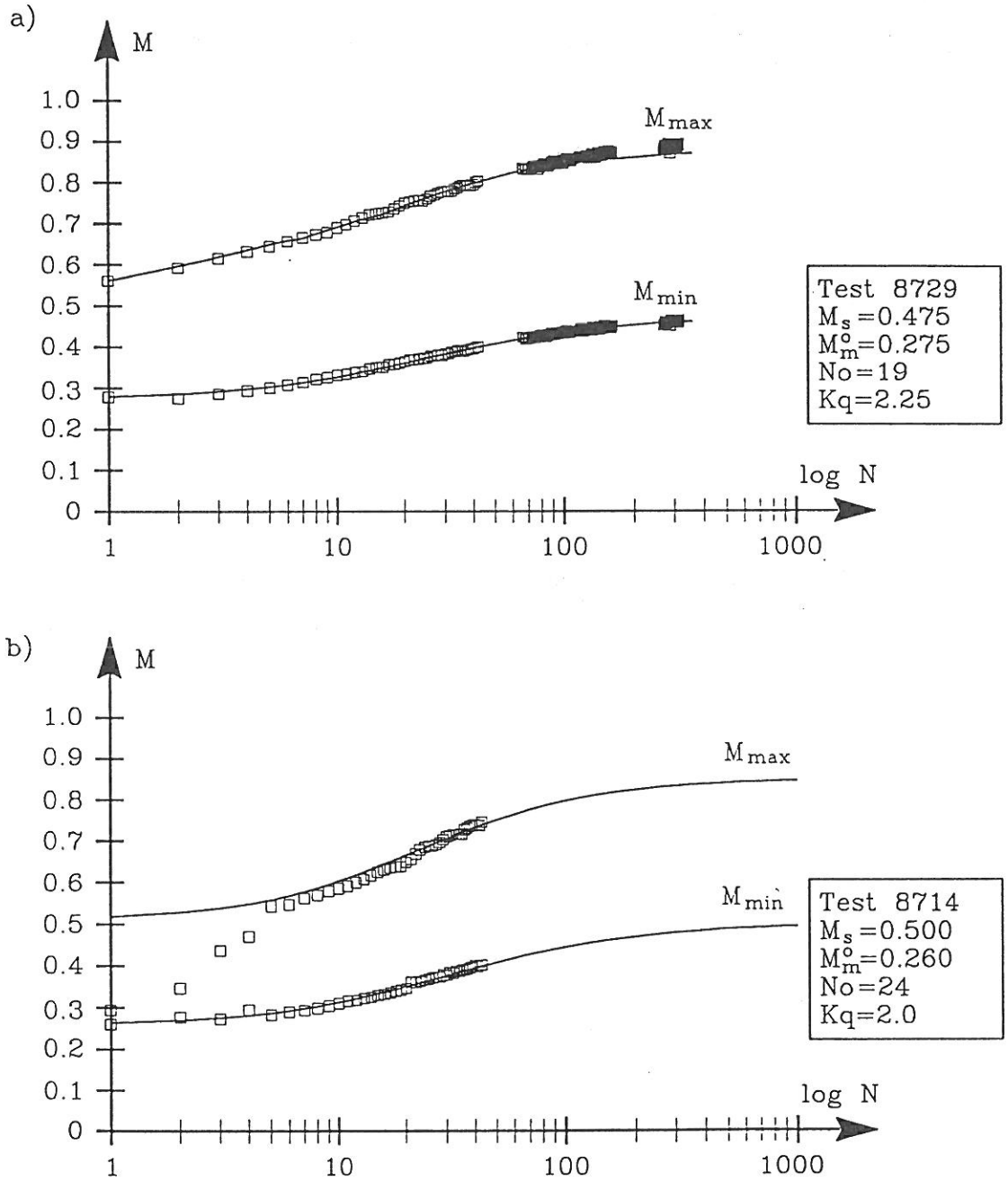

Figure 12. In Mobilizing, tests No 8729 and No 8714, the observed development of M_m and M_{max} has been compared to the development calculated after (9) and (30). In b) a prediction has been carried out since the test was stopped after 45 cycles.

Goodness of M_m fit

In figures 12 – 15 the variation of M_m has been determined according to the established theory compared to the stress development from tests representing the 4 phenomena Mobilization (Figure 12a and b), Instant Stabilization (Figure 13a and b), Stabilization (Figure 14a and b) and Cyclic Liquefaction (Figure 15a and b). The parameters, applied when simulating the individual tests, are shown in the figures. The applied parameters are identical to the values in Tables 1 and 2.

A prediction has been carried out in Figure 12b, having interrupted the Mobilization test after 45 cycles. The stress development has not been determined entirely and M_s is unknown. The stress development in the test has been simulated, applying equations (9) and (10). M_m° has been calculated from p'_s, q'_s. $M_s = 0.5$ and $\ell = 1.25$. N_0 has been determined from equation (23). The calculated stress development is observed to be identical with the measured one.

In the cyclic fatigue theory it is assumed that Instant Stabilization can be treated as Mobilization, when M_m° is determined from the stress state after the initial half cycle. Figure 13a and b show that this procedure is a good approximation.

The failure indicator M_{cl-} was introduced in section 1 in order to be able to simulate the stress/strain development until failure. In Figure 15a and b, M_m is marked • by the cycles where $M_{min} \leq M_{cl-}$. The equation system describes the development of M_m all the way to failure, and in accordance with the cyclic fatigue theory failure develops as soon as $M_{min} \leq M_{cl-}$.

In all 8 tests the simulated stress development is observed to be identical to the measured one. Consequently, it can be concluded that the chosen procedure in parameter determination and the theoretical assumptions are valid, since the mean mobilization can be described for the 4 observed phenomena.

However, it is somewhat surprising that no amplitude dependence has been demonstrated during the determination of the parameters N_0 and ℓ. In practice this means that a $q'_{cyk} \approx 0$ will result in as large a buildup/reduction of pore pressure per cycle as a q'_{cyk}, which causes failure in the specimen after a few cycles. It is obvious that this cannot be correct. The determination of N_0 and ℓ has been carried out on the basis of only one test series performed at a high amplitude level (k_q M_m). The amplitude ratio k_q is observed to be placed in the interval $1.5 < k_q < 2.5$ (Tables 1 and 2), and the test series covers the stress area $M_m^\circ > 0.2$, see Figure 11. Thus, the performed test series must be supplemented with test series describing the development at lower amplitude levels. If $\ell = 1.25$ is maintained, $N_0(M_m^\circ, k_q)$ and the variation of N_0 must be described in one of the following two methods:

- $N_0\,(M_m^\circ) = \Psi\,(k_q)\left(\dfrac{1 - M_m^\circ}{M_m^\circ}\right)$, corresponding to a swarm of curves in Figure 11.

- $N_0\,(k_q M_m^\circ) = \Psi\left(\dfrac{1 - k_q M_m^\circ}{k_q M_m^\circ}\right)$

Future test series must determine which of the two expressions gives the best description. N_0 described by equation (23) corresponds to a development of M_m, which is close to maximum.

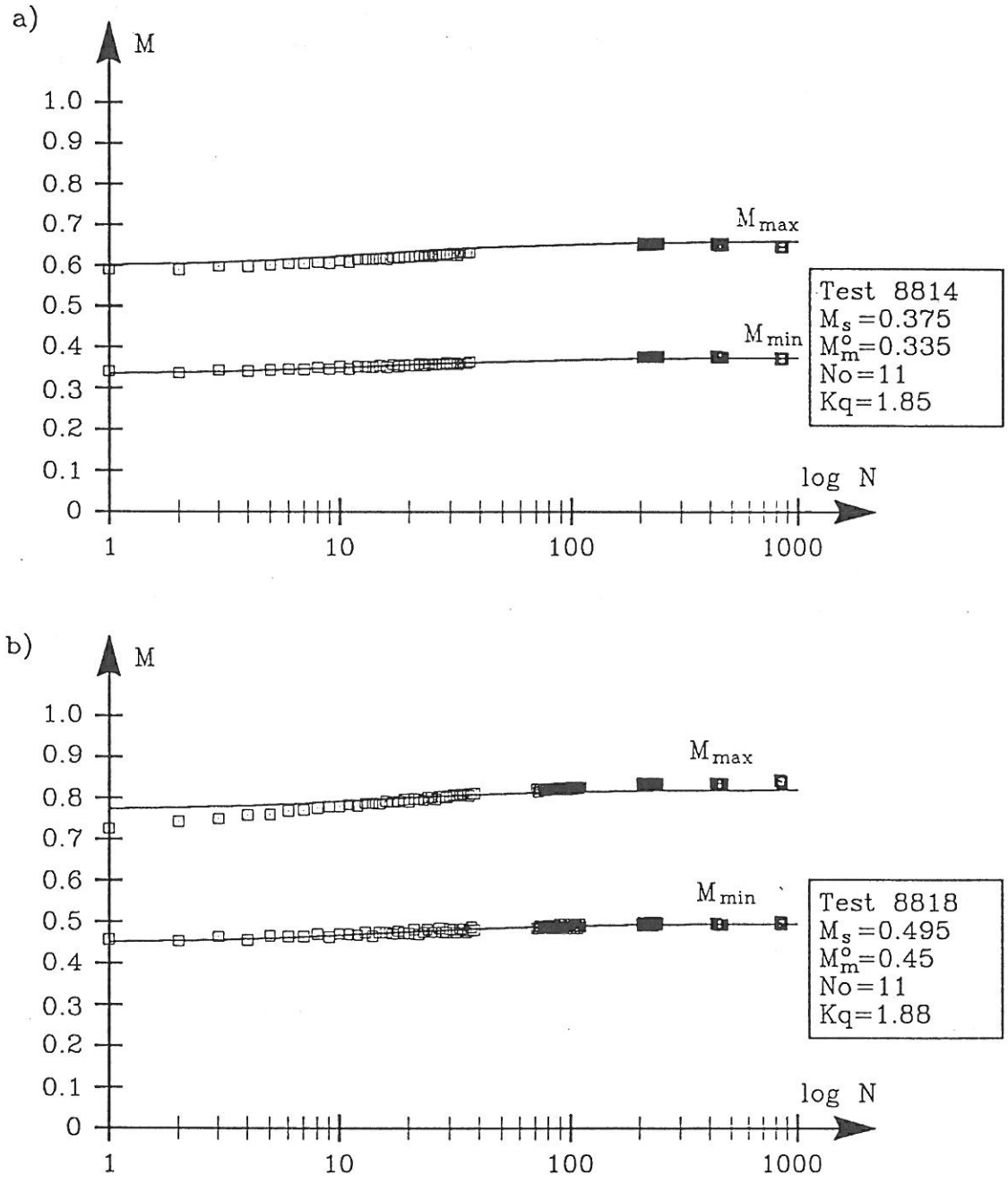

Figure 13. In Instant Stabilization, tests No 8814 and No 8818, the observed development of M_m and M_{max} has been compared to the development calculated after (9) and (30).

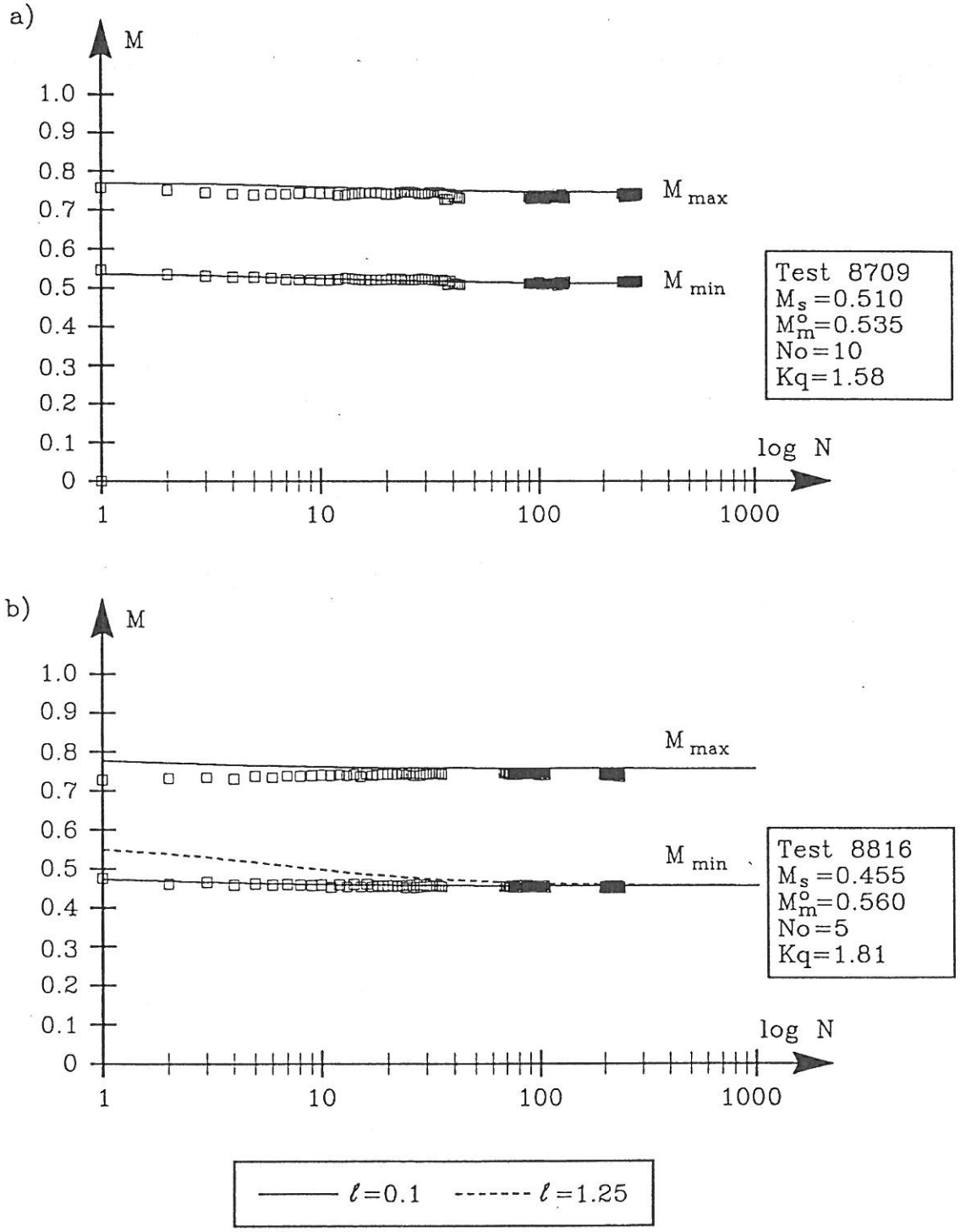

Figure 14. In Stabilization, tests No 8709 and No 8816, the observed development of M_m and M_{max} has been compared to the development calculated after (9) and (30).

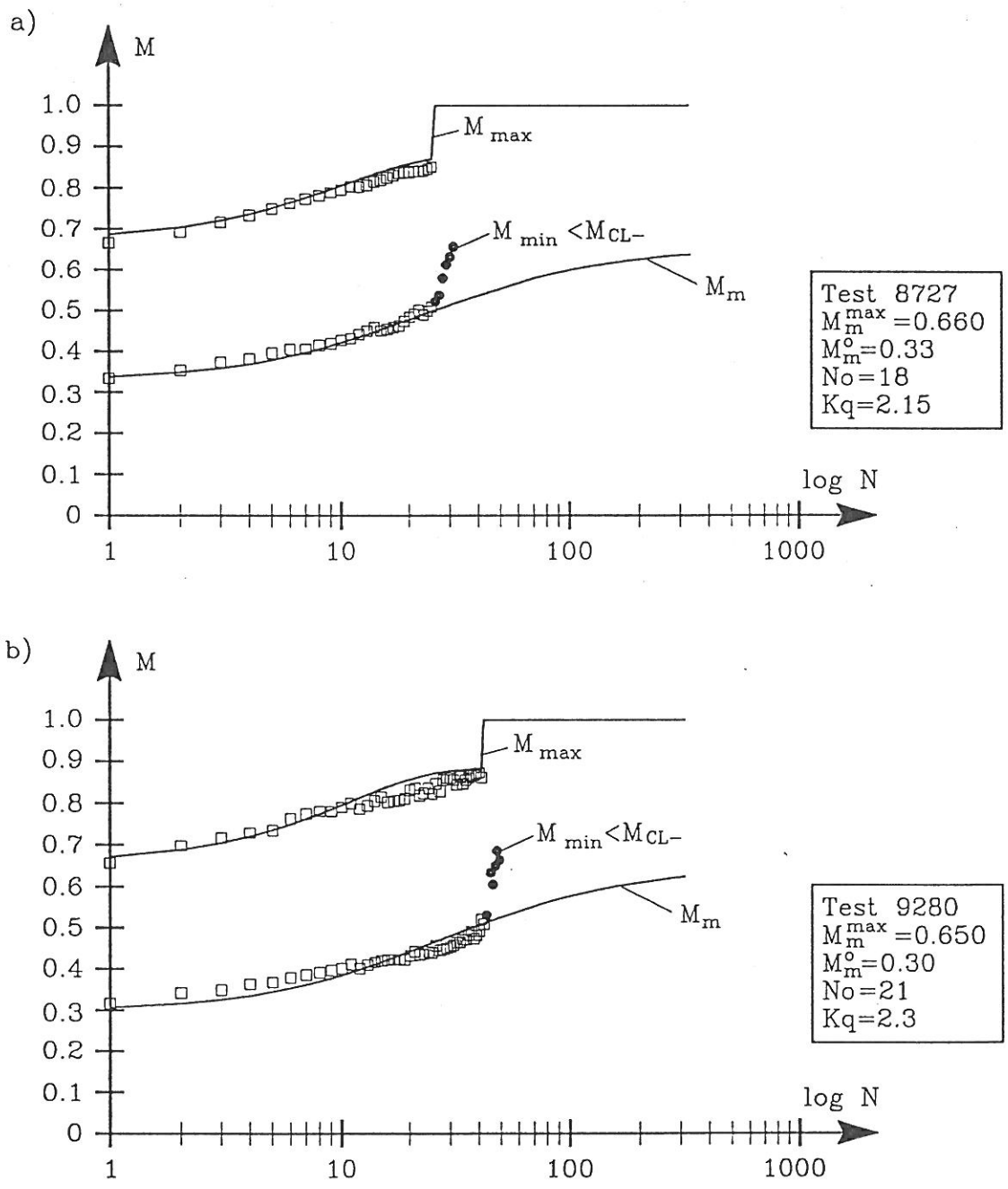

Figure 15. In Cyclic Liquefaction, tests No 8727 and No 9280, the observed development of M_m and M_{max} has been compared to the development calculated after (9) and (30).

1.3 Description of M_{max} and M_{min}

First Order Theory

In /Ibsen, L.B., Jacobsen, M. 1991/ it was suggested that

$$M_{max} = k_q M_m \tag{24}$$

It is evident from equations (18) - (22) that α is assumed to be 0, corresponding to an ideal elastic material. This gives a simple but extremely operational equation system to describe the stress development under a given cyclic loading. If M_m is determined from equation (4) it is easy to determine M_{max} from equation (24) and M_{min} can be determined

$$M_{min} = (2 - k_q)\, M_m \tag{25}$$

since

$$M_{min} = M_m - M_{cyk}$$

$$M_{cyk} = k_q M_m - M_m$$

If the first order theory is applied Figure 2 shows that failure occurs if

$$k_q M_m \geq 1 + |M_{cl^-}| \tag{26}$$

Figures 16 and 17 show the consequence of describing the stress development, applying the first order theory. Observing the last cycle in the tests in Tables 1 and 2, M_{max} has been plotted in Figure 16 as a function of $(k_q \cdot M_m)$, and M_{min} plotted in Figure 17 is a function of $(2 - k_q)\, M_m$. M_{max} and M_{min} have been calculated from the first order theory, see Figures 16 and 17, corresponding to the line of 45°, which has also been plotted. Figure 17 shows that the first order theory describes the development of M_{min}, since M_{min} observed and M_{min} calculated are in agreement. Since q'_m is placed between the characteristic lines in extension and compression, respectively, the first order theory is a good assumption, and M_{min} can be determined from equation (25). However, the first order theory results in an overestimation of M_{max}. In a given dimension situation it would be safe to estimate M_{max} from the first order theory.

If the stress/strain development is to be described it is, however, necessary to determine the correct development of M_{max}, i.e. it must be taken into consideration that the inclination of the stress cycles becomes smaller when the stress variation approaches failure. The second order theory, described in the following section, describes this development and ought to be applied in the cases where the stress/strain development is to be modelled.

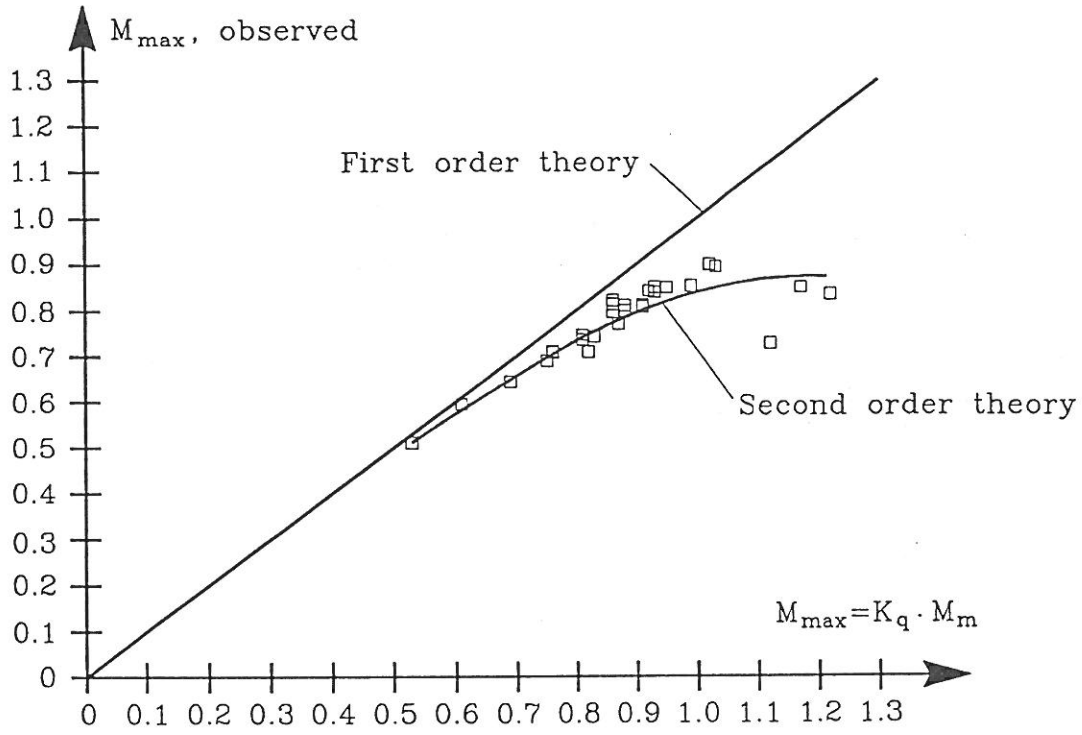

Figure 16. The figure shows M_{max} observed during the last cycle in the tests in Tables 1 and 2. These values are compared with M_{max} calculated after (24) and (30), First and Second Order, respectively.

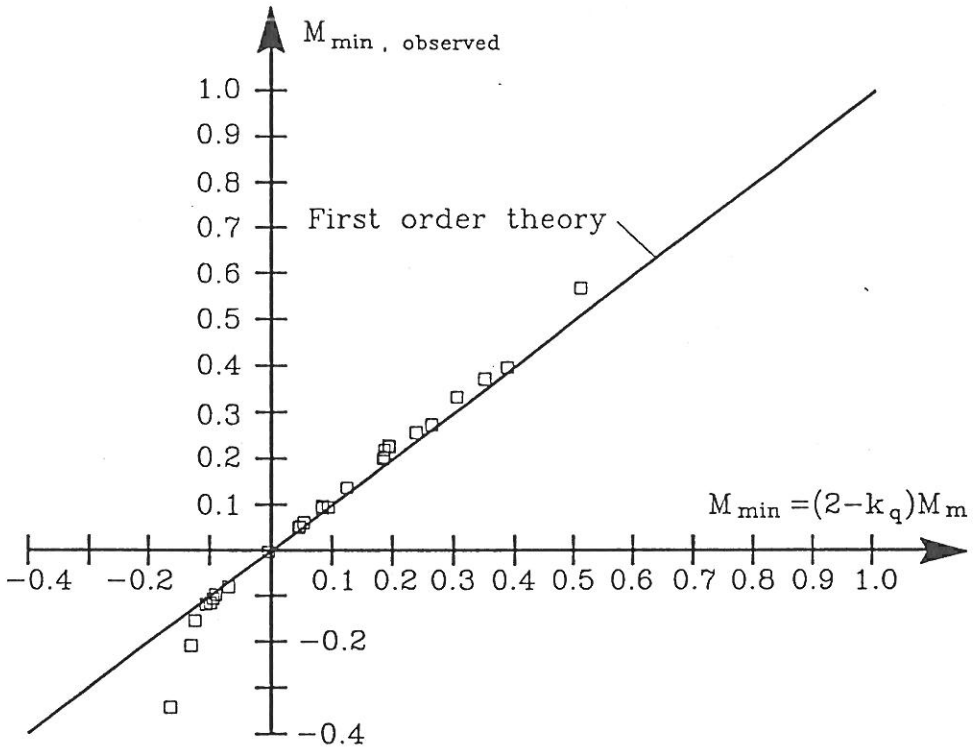

Figure 17. The figure shows that M_{min} is observed during the last cycle in the tests in Tables 1 and 2. These values are compared with M_{min} calculated after the First Order Theory, equation (25).

Second order theory

Generally M_{max} can be described as

$$M_{max} = M_m + M_{cyk} \tag{27}$$

If the correct development of M_{max} is to be determined it is necessary to take the inclination of the stress cycle into consideration, i.e. α, see Figure 18. M_{cyk} is a function of α and the following correlation can be established:

$$M_{cyk} = \frac{q'_{cyk}}{q'_f(p'_m) + \Delta q'_f} \tag{28}$$

$$\text{where } \Delta q'_f = q'_{cyk} tan\alpha tan\beta$$

$$\text{since } \Delta q'_f = \Delta p' tan\beta$$

$$\Delta p' = q'_{cyk} tan\alpha$$

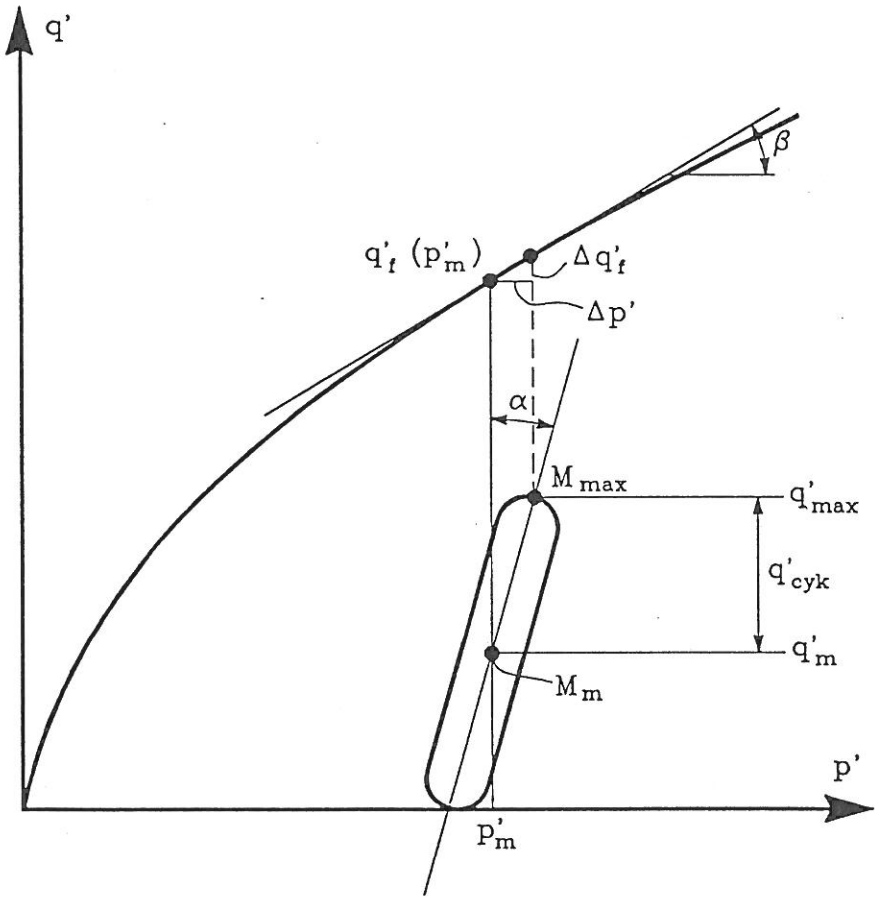

Figure 18. Determination of M_{max} using the Second Order Theory.

If the amplitude ratio k_m is introduced – defined from the normalized stresses as

$$k_m = \frac{M_m + M_{cyk}}{M_m} \tag{29}$$

and if equation (29) is inserted in (27), M_{max} can be expressed as

$$M_{max} = k_m M_m \tag{30}$$

like the first order theory.

Contrary to k_q, k_m is not a constant but a function of α. If α is assumed only to depend on the maximum stress level and not on the stress variation, which has led to the given level, k_m must be a function of M_{max}. The following boundary condition for k_m can be established

$$\begin{aligned} k_m &= k_q \quad \text{for} \quad \alpha = 0 \\ k_m &\to k_m^{min} \quad \text{for} \quad M_{max} \to 1 \end{aligned} \tag{31}$$

where k_m^{min} is a constant.

Normalizing k_m as far as k_q is concerned the following is obtained

$$\frac{k_m}{k_q} = 1 \quad \text{for} \quad \alpha = 0$$

Since the maximum stress level M_{max}, which k_m is a function of, is unknown, the variation of k_m is described by applying the relative stress level $k_q M_m$. Figure 19 shows the observed values of k_m/k_q as a function of $k_q M_m$. k_m/k_q describes a descending curvature with relative small scattering. In the figure 7818 cycles have been plotted and they represent the 17 tests marked **) in Tables 1 and 2. The results verify the assumption

- that α only depends on the maximum stress level

thus, it must be reasonable to assume k_m^{min} = constant for $M_{max} \to 1$.

$$\frac{k_m}{k_q} \to \frac{k_m^{min}}{k_q} \quad \text{for} \quad M_{\max} \to 1 \tag{32}$$

The boundary condition for the stress level can – according to (26) – be described as

$$k_q M_m \to (1 + |M_{cl-}|) \quad \text{for} \quad M_{max} \to 1 \tag{33}$$

A simple description of k_m/k_q as function of the stress level has been found to

$$\frac{k_m}{k_q} = 1 - \left(1 - \frac{k_m^{min}}{k_q}\right) \cdot f\,(k_q M_m) \tag{34}$$

The difference $\left(1 - \frac{k_m^{min}}{k_q}\right)$ describes the variation in k_m while the function $f(k_q M_m)$ describes the curvature. In order to make (34) fulfill the boundary conditions (32) and (33) $f(k_q M_m)$ must be worked out so that

$$\begin{aligned} f(k_q M_m) &\to 0 \quad \text{for} \quad k_q M_m \to 0 \\ f(k_q M_m) &\to 1 \quad \text{for} \quad k_q M_m \to 1 + |M_{cl-}| \end{aligned} \tag{35}$$

A function, which complies with these conditions has been found to

$$f(k_q M_m) = \left(\frac{k_o + k_q M_m}{(k_q M_m)^{max} + k_o} \right)^{\beta} \tag{36}$$

where k_o and β are constants determining the curvature and $(k_q M_m)^{max} = 1 + |M_{cl}-|$. (36) fulfills the boundary conditions from (35) only if $k_o << 1 + |M_{cl}-|$.

Since M_{max} is determined from (30) the simple but extremely operative equation system from the first order theory has been transferred to the second order theory. The procedure is almost identical except for an extra loop, since k_m – contrary to k_q – must be determined in each cycle. In order to determine k_m, the parameters k_o and β must be determined. M_{min} is determined, like in the first order theory, from

$$M_{min} = (2 - k_q) \cdot M_m$$

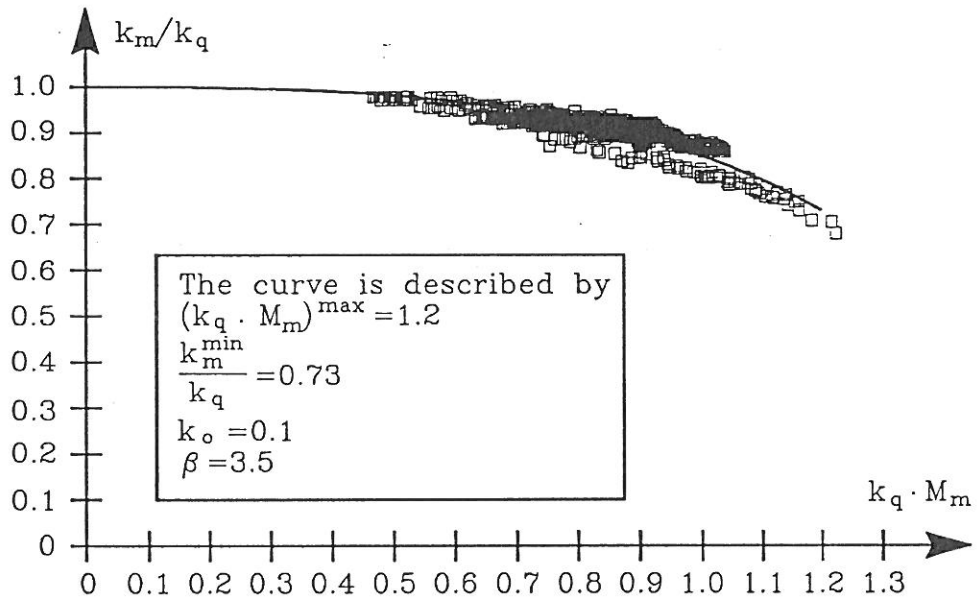

*Figure 19. k_m/k_q is shown as a function of the relative stress level for each cycle in the tests which are marked ** in Tables 1 and 2. In the figure 7818 cycles are plotted.*

Parameter determination

Parallel to the description of M_m the equation system, describing the variation of k_m with the stress level, is build in such a way that the parameter fitting can be carried out in each individual test. However, it is a requirement that the test covers a large part of the stress area corresponding to Cyclic Liquefaction tests with a low initial mobilization degree M_m°. The test series performed in connection with this project do not contain tests which comply with this requirement.

The tests marked **) in Tables 1 and 2 have been applied in order to cover the entire stress area. For each cycle in these tests k_m/k_q has been plotted as a function of the stress level given by $k_q M_m$, see Figure 19. k_m has been determined from the observed values of M_{max}/M_m in each cycle, while k_q has been determined from (19).

Figure 19 shows a curve which has been plotted by means of (34) and (36). The curve has been determined by the method of least squares and describes the development of k_m as an average of the 7818 cycles representing 17 tests. The boundary values $(k_q M_m)^{max}$ and k_m^{min} are no longer the boundary conditions, which the individual test moves towards, but describe the boundary condition for the curve. In order to determine the curve the following 4 unknown parameters $(k_q M_m)^{max}$, $k_m^{min}/k_q, k_0$, and β must be determined. Like the parameter determination in section 2 the 4 parameters converge with different speeds and cannot be determined by only one curve fitting procedure.

Determination of $(k_q M_m)^{max}$

The boundary condition

$$(k_q M_m)^{max} = 1 + |M_{cl-}|$$

in (36) governs the limitation of the loaded stress space. From (6) and Figure 2 it is evident that M_{cl-} is a function of p'_{cl-}, because the characteristic line is straight and the failure condition is curved. Since the 17 tests from Figure 19 have been carried out with different values of k_q, $(k_q M_m)^{max}$ must be determined from an average in order to describe the stress area covered in the test series. Figure 16 shows that M_{max}, observed during the last cycle in the tests in Tables 1 and 2, is shown as a function of $k_q M_m$. If $(k_q M_m)^{max} = 1.2$ is chosen, the stress space represents the test series.

Determination of k_o

In order to fulfill the boundary conditions given by (35), k_o must be $<< 1+|M_{cl-}|$. Forthwith k_o could be omitted and (36) would still fulfill the boundary conditions. However, k_o has been introduced in order to be able to model the curvature for $k_q M_m \rightarrow 0$. In this test series the smallest value of $k_q M_m = 0.45$ and consequently k_o is insignificant. In this case k_o is chosen to be 0.1 and future test series must determine if it can be omitted.

Determination of k_m^{min}/k_q and β

With these values of $(k_q M_m)^{max}$ and k_o, k_m^{min}/k_q and β have been determined by the method of least squares

$$k_m^{min}/k_q = 0.73$$

$$\beta = 3.5$$

With these values M_{max} has been calculated during the last cycle in the tests in Tables 1 and 2. The results are plotted in Figure 16 as the curved line. Compared to the first order theory it is observed that the second order theory describes the development of M_{max} regardless of whether it is the phenomena Cyclic Liquefaction, Mobilization, Stabilization or Instant Stabilization.

Goodness of M_{max} fit

Like the variation of M_m, M_{max} has been determined from the second order theory and compared with the stress development in tests representing the 4 phenomena Mobilization, Instant Stabilization, Stabilization and Cyclic Liquefaction in Figures 12 - 15.

Figure 16 shows that the second order theory is able to describe the final condition in the tests in Tables 1 and 2. Figures 12 - 15 show that the second order theory is also able to simulate the stress development throughout the test. Considering that the parameters determining k_m are not fitted in each individual test, the development of M_{max} is described extremely well in all test types.

This must indicate that α is only a function of the stress level and that the approximation

$$\begin{aligned} \frac{k_m^{min}}{k_q} &= 0.73 \\ (k_q M_m)^{max} &= 1.2 \end{aligned} \tag{37}$$

represents the stress space. Since (37) determines k_m for $M_{max} \rightarrow 1$, the largest deviation between the calculated M_{max} and the observed M_{max} can be expected to take place in tests developing Cyclic Liquefaction. Regarding the tests in Figure 15 it is observed that (34) and (36) simulate the development of M_{max}, even when $M_{max} \rightarrow 1$.

Like the simulation of M_m in Figure 12b, where the stress development is done by prediction, the estimated variation is seen to describe the observed one. The cyclic stress variation is observed to be applied with increasing amplitude to reach the chosen valve only in cycle no. 5. In spite of this, the second order theory is observed to describe the development of M_{max}.

The approximations (37) can be applied in tests where the stress space is limited by $p' <$ 100 kPa. Whether the approximations can be applied in tests covering a larger stress space must be determined in test series dealing with the stress development around the failure condition, i.e. tests with a low initial mobilization degree and where Cyclic Liquefaction is developed. This way the individual test can be modelled/fitted. Thus, it can be determined if k_m^{min} should be described as a function of $(k_m M_m)^{max}$.

1.4 Closing remarks

As seen in Figures 12 - 17 it has been possible to work out a fatigue model, which models the phenomena observed during cyclic loading. Compared to the model described in /Jacobsen, M. and Ibsen, L.B. 1991/, the stress variations moving towards failure can now be modelled. The model has been made general since it is also possible to use it to describe test results where the stable cyclic condition does not occur, i.e. tests where Cyclic Liquefaction or Necking is developed. Furthermore, the model can be used to model test results from tests performed on specimens with double height of the specimen. In equation (9) M_m^{∞} will always be equal to M_m^{max}, see (11). The parameters, applied in the model to describe the development of M_m and k_m, will not be identical with the result found in this paper when testing specimens with double height are used.

The parameter determinations in this chapter have only been performed with a relative density of $I_D = 0.78$ and an amplitude condition k_q, which determines the maximum development of the stress variation. Thus, some research needs to be carried out in order to explain

- M_s's dependence on the density
- N_o's variation with k_q
- If k_m^{min} should be described as a function of $(k_m M_m)^{max}$.

If the model is to be used as a basis for geotechnical decisions, the entered parameters must be determined in each case until more experience is available.

In order to describe how the fatigue model might be applied in a geotechnical decision process, a possible procedure to be used in a stability investigation of a gravitation construction is shown in the paper "Application of the cyclic fatigue model".

AGEP: Environmental Engineering papers

12 Lade, P.V., Ibsen, L.B. (1997). A study of the phase transformation and the characteristic lines of sand behaviour. Proc. Int. Symp. on Deformation and Progressive Failure in Geomechanics, Nagoya, Oct. 1997, pp. 353-359. Also in *AAU Geotechnical Engineering Papers*, ISSN 1398-6465 R9702.

13 Bødker, L., Steenfelt, J.S. (1997). Vurdering af lodrette flytningsamplityder for maskinfundament, Color Print, Vadum (Evaluation of displacement amplitudes for printing machine foundation; in Danish). *AAU Geotechnical Engineering Papers*, ISSN 1398-6465 R9706.

14 Ibsen, L.B., Steenfelt, J.S. (1997). Vurdering af lodrette flytningsamplityder for maskinfundament Løkkensvejens kraftvarmeværk (Evaluation of displacement amplitudes for gas turbine machine foundation; in Danish. *AAU Geotechnical Engineering Papers*, ISSN 1398-6465 R9707.

15 Steenfelt, J.S. (1997). National R&D Report : Denmark. *Seminar on Soil Mechanics and Foundation Engineering R&D*, Delft 13-14 February 1997. pp 4. Also in *AAU Geotechnical Engineering Papers*, ISSN 1398-6465 R9708.

16 Lemonnier, P. and Soubra, A. H. (1997). Validation of the recent development of the displacement method - geogrid reinforced wall. *Colloquy EC97 on the comparison between experimental and numerical results*, Strasbourg, France. Vol.1, pp. 95-102. Also in *AAU Geotechnical Engineering Papers*, ISSN 1398-6465 R9712.

17 Lemonnier, P. & Soubra, A. H. (1997). Recent development of the displacement method for the design of geosynthetically reinforced slopes - Comparative case study. *Colloquy on geosynthetics, Rencontres97, CFG*, Reims, France, Vol. 2, pp. 28AF-31AF (10pp). Also in *AAU Geotechnical Engineering Papers*, ISSN 1398-6465 R9713.

18 Lemonnier, P., Soubra, A. H. & Kastner, R. (1997). Variational displacement method for geosynthetically reinforced slope stability analysis : I. Local stability. Geotextiles and Geomembranes 16 (1998) pp 1-25. Also in *AAU Geotechnical Engineering Papers*, ISSN 1398-6465 R9714.

19 Lemonnier, P., Soubra, A. H. & Kastner, R. (1997). Variational displacement method for geosynthetically reinforced slope stability analysis : II. Global stability. Geotextiles and Geomembranes 16 (1998) pp 27-44. Also in *AAU Geotechnical Engineering Papers*, ISSN 1398-6465 R9715.

20 Ibsen, L.B. (1998). Analysis of Horizontal Bearing Capacity of Caisson Breakwater. 2nd PROVERS Workshop, Napels, Italy, Feb. 24-27-98. Also in *AAU Geotechnical Engineering Papers*, ISSN 1398-6465 R9802.

21 Ibsen, L.B. (1998). Advanced Numerical Analysis of Caisson Breakwater. *2nd PROVERS Workshop*, Napels, Italy, Feb. 24-27-98. Also in *AAU Geotechnical Engineering Papers*, ISSN 1398-6465 R9803.

22 Ibsen, L.B., Lade P.V. (1998). The Role of the Characteristic Line in Static Soil Behavior. *Proc. 4th International Workshop on Localization and Bifurcation Theory for Soil and Rocks*. Gifu, Japan. Balkema 1998. Also in *AAU Geotechnical Engineering Papers*, ISSN 1398-6465 R9804.

AGEP: Environmental Engineering papers

23 Ibsen, L.B., Lade, P.V. (1998). The Strength and Deformation Characteristics of Sand Beneath Vertical Breakwaters Subjected to Wave Loading. 2nd PROVERS Workshop, Napels, Italy, Feb. 24-27-98. Also in *AAU Geotechnical Engineering Papers*, ISSN 1398-6465 R9805.

24 Steenfelt, J.S., Ibsen, L.B. (1998). The geodynamic approach - problem or possibility? Key Note Lecture, *Proc. Nordic Geotechnical Meeting, NGM-96, Reykjavik, V*ol 2, pp 14. Also in *AAU Geotechnical Engineering Papers*, ISSN 1398-6465 R9809.

25 Lemonnier, P., Gotteland, Ph. and Soubra, A. H. (1998). Recent developments of the displacement method. *Proc. 6th Int. Conf. on Geosynthetics. Atlanta, USA*, Vol 2, pp 507-510. Also in *AAU Geotechnical Engineering Papers*, ISSN 1398-6465 R9814.

26 Praastrup, U., Jakobsen, K.P., Ibsen, L.B. (1998). On the choice of strain measures in geo-mechanics. 12th Young Geotechnical Engineers Conference, Tallin, Estonia. *AAU Geotechnical Engineering Papers*, ISSN 1398-6465 R9815.

27 Ibsen, L.B. (1998). The mechanism controlling static liquefaction and cyclic strength of sand. Proc. Int. Workshop on Physics and Mechanics of Soil Liquefaction, Baltimore. A.A.Balkema, ISBN 9058090388, pp 29-39. Also in *AAU Geotechnical Engineering Papers*, ISSN 1398-6465 R9816.

28 Ibsen, L.B., Jakobsen, K.P. (1998). Limit State Equations for Stability and Deformation. *AAU Geotechnical Engineering Papers*, ISSN 1398-6465 R9828.

29 Praastrup, U., Ibsen, L.B., Lade P.V. (1999). Presentation of Stress Points in the Customised Octahedral Plane. Published in *Proc. 13th ASCE Engineering Mechanics Division Conference,* June 13-16, 1999, Baltimore, USA, 6 pages. *AAU Geotechnical Engineering Papers*, ISSN 1398-6465 R9906.

30 Praastrup, U., Ibsen, L.B., Lade P.V. (1999). A Generic Stress Surface Introduced in the Customised Octahedral Plane. Proc. *7th Int. Symp. on Numerical Models in Geomechanics,* Graz, Austria, Sept. 1.-3. 1999. Balkema, Rotterdam ISBN 90 5809 095 7, pp 71-76. *AAU Geotechnical Engineering Papers*, ISSN 1398-6465 R9907.

31 Ibsen, L.B., Lade P.V. (1999). Effects of Nonuniform Stresses and Strains on Measured Characteristic States. Proc. *2nd Int. Symp. Pre-failure Deformation Characteristics of Geomaterials*, IS Torino 99, Sept. 26.-29.1999, pp 897-904. *AAU Geotechnical Engineering Papers*, ISSN 1398-6465 R9908.

32 Jakobsen, K.P., Praastrup, U., Ibsen, L.B. (1999). The influence of the stress path on the characteristic stress state. Proc. *2nd Int. Symp. Pre-failure Deformation Characteristics of Geomaterials*, IS Torino 99, Sept. 26.-29.1999, pp 659-666. *AAU Geotechnical Engineering Papers*, ISSN 1398-6465 R9909.

33 Praastrup, U., Jakobsen, K.P., Ibsen, L.B. (1999). Two Theoretically Consistent Methods for Analysing Triaxial Tests. Published in *Computers and Geotechnics,* Vol. 25(1999), pp. 157-170. *AAU Geotechnical Engineering Papers*, ISSN 1398-6465 R9912.

34 Ibsen, L.B. (1999). Cyclic Fatigue Model. *AAU Geotechnical Engineering Papers*, ISSN 1398-6465 R9916.